FACTA UNIVERSITATIS
Series: **Electronics and Energetics** Vol. 32, N^{o} 2, June 2019, pp. 303-314
https://doi.org/10.2298/FUEE1902303P

THE INFLUENCE OF BUSBARS CONNECTION ON FUSELINK TEMPERATURE AT FAST FUSES

Adrian Plesca

Gheorghe Asachi Technical University of Iasi, Faculty of Electrical Engineering, Romania

Abstract. *The paper, based on three-dimensional thermal modelling and simulation finite element method software package, presents a comparison between the thermal behaviour of a fast fuse without busbar terminals and the one with these busbars mounted on it. The maximum fuselink temperature is lower in the second case when the thermal model had taken into consideration the busbar connections, actually, the real situation. Also, a thermal analysis for different type of load variations has been done in both cases of the fast fuse geometry with and without busbar terminals.*

Key words: *busbars, fast fuses, fuselinks, heating, thermal modelling and simulations*

1. INTRODUCTION

At the first sight, the electric fuse manufacture and its working principle don't seen a hardly gain insight into matters, in fact this device operating is very complex, [1, 2]. Choosing the right fuses for the safety purposes implies anyway some criteria and also tests methodologies in order to prevent fuse failure. [3]. Electric fuses operation is widely studied from the point of view theoretical, experimental and modelling aspects [4, 5]. Fuses for power semiconductors are used in different domain area, starting from the distribution network to special applications, such as: automotive [6], adjustable speed drive [7], photovoltaic systems [8], power substations [9] or microgrids [10].

Different models of fuses were developed usually based on a mathematical representation of the arc physics. These models include transient heating and fusion of notched strip elements in sand, arc ignition, and subsequent burn-back, radial expansion of the arc channels due to fusion of the sand, merging of adjacent arcs, and many other second-order effects [11-13]. Different parameters such as thermal distribution, thermal flux, and electrical potential in all fuse parts are obtained [13].

Fast fuses for power semiconductor protection have been continually developed, in general on the basis of experimental methods. Because the processes which govern the operation of fuselinks are many and complex, its analysis is very complicated and several

Received December 14, 2018; received in revised form February 20, 2019
Corresponding author: Zoran Stanković
Gheorghe Asachi Technical University of Iasi, Faculty of Electrical Engineering, Romania
(E-mail: aplesca@ee.tuiasi.ro)

simplifying assumptions are required. The very complicated situation is that of the prearcing times longer than those which correspond with an adiabatic process, because the current densities in the fuselinks are not constant over their cross-section or along their lengths due to the presence of the restrictions, [14, 15]. In addition, resistivity increases as the fuselink temperature rises, and the effects of various component parts, like fine-grain filler, outer body, end caps, connecting cables or busbars must be considered in temperature distribution analysis, [16].

Fuses for power semiconductors have been investigated in [17-20]. In [21] inverter design requirements for safe fuse blowing are investigated. The effects of differing fuse characteristics and the influence on semiconductors during fuse interruption are evaluated in theory and with a practical setup. Design hints for fuse locations and selection have been presented. Along with the main grid protection, hybrid AC/DC microgrids require also special attention for their protection [22]. Energy storage systems are studied from the point of view of their protection in order to reduce the incident energy of the arc flash. Use of fast-acting fuses is effective, reducing the incident energy to low values [23].

This paper aims to study the influence of the busbar connections of the fast fuse from temperature distribution point of view, using a specific software package based on Finite Element Method, in order to model and simulate in steady-state conditions their complex thermal behaviour.

2. THERMAL ANALYSIS OF FAST FUSES

In the case of variable loads or transient conditions, there is the posibility to set up an equivalent thermal circuit where every section of the fast fuse assembly is represented by its thermal resistance and thermal capacity taking into account that in every section is accumulated a part of the heat released in the fuselink. The most important elements to be taken into consideration in the equivalent thermal circuit are: the fuselink, the quartz sand, the ceramic body of the fuse and the busbar connections. In Fig. 1 is presented the equivalent thermal circuit considering in a simplified way the concentrated parameter of the fast fuse assembly.

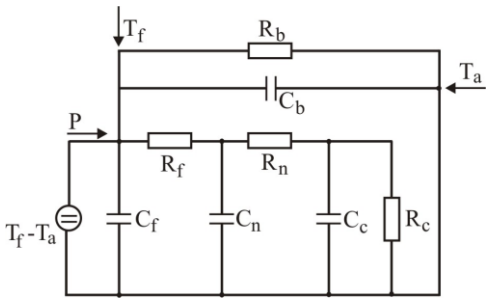

Fig. 1 Equivalent thermal circuit of the fast fuse assembly

The notations in the figure have the following meaning: R_f – thermal resistance of the fuselink, R_n – thermal resistance of the quartz sand, R_c – thermal resistance of the ceramic body of the fuse and R_b – thermal resistance of the busbar connection. Similarly, C_f is the

thermal capacity of the fuselink, C_n – thermal capacity of the quartz sand, C_c – thermal capacity of the fuse ceramic body and C_b – thermal capacity of the busbar. The products between thermal resistance and capacity allow to compute the thermal time constant, i.e. R_fC_f – thermal time constant of the fuselink. This is an important parameter which leads to calculate the time after which the fuselink reaches the steady-state temperature (after approximate 5 thermal time constant). The values of the thermal resistances and capacities can be roughly calculated from the dimensions and the characteristics of the materials which the assembly is made of. The correspondence between thermal parameters with physical components of the fast fuse, is shown in Fig. 2.

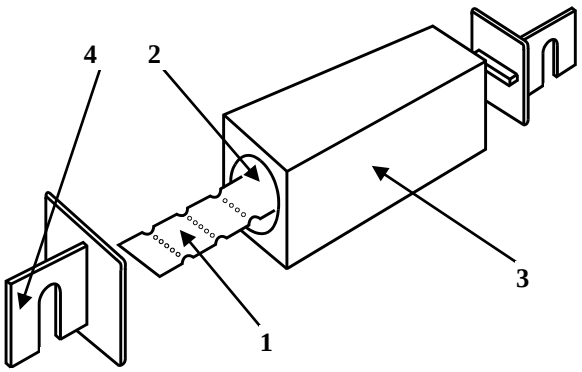

Fig. 2 Main components of the fast fuse (1 – fuselink; 2 – sand qurtz; 3 – ceramic body; 4 – terminal for busbar connection)

For the thermal computation in the transient regime it can be defined the fast fuse response when a step power is applied, Fig. 3, which is called transient thermal impedance $Z_{th}(t)$, and usually it is experimentally determined:

$$Z_{th}(t) = \frac{\Delta\theta(t)}{P} \tag{1}$$

where:

$Z_{th}(t)$ is the transient thermal impedance;

$\Delta\theta(t)$ – fuselink temperature rise;

P - step pulse power.

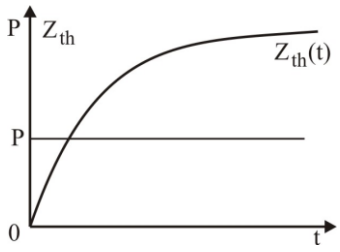

Fig. 3 Transient thermal impedance

$Z_{th}(t)$ can be considered as representing the possibilities of evacuation and storage of heat in the fuselink at the moment in time t. Under constant heating and cooling conditions, the temperature of a homogeneous body of small size will have an exponential variation to a steady-state value, determined by the caloric power released into the body and by the body-to-ambient thermal resistance. Thus, for $Z_{th}(t)$, it is convenient an approximation by sum of exponentials:

$$Z_{th}(t) \approx \sum_{j=1}^{k} r_j \left(1 - e^{-\frac{t}{T_j}} \right) \tag{2}$$

The k number of the exponential functions, the number of the time constants $T_j = r_j C_j$, and the number of the thermal resistances r_j, do not correspond to the number of the elements and of the calculated values from the characteristics and the dimensions of the materials of which the fast fuse is made of. Instead, they are generally determined directly from the curve of $Z_{th}(t)$.

The thermal response of a single element can be extended to a complex system, such as a fast fuse with or without busbar connections, whose thermal equivalent circuit comprises a ladder network of the separate resistance and capacitance terms. Transient thermal impedance data, derived on the basis of a step input of power, can be used to calculate the thermal response of fast fuses for a variety of one-shot and repetitive pulse inputs. Further on, the thermal response for commonly encountered situations, Fig. 4, has been computed and is of great value to the circuit designer who must specify a fast fuse and its characteristics [24].

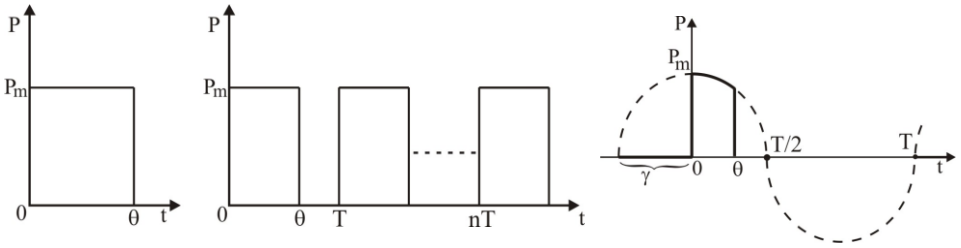

a) b) c)

Fig. 4 Types of thermal load (a – rectangular pulse; b – rectangular pulse series; c – partial sinusoidal pulse)

The time variation of the rectangular pulse input power is shown in Fig. 4a and its expression is given by the equation (3).

$$P(t) = \begin{cases} P_m \ \ if \ \ 0 < t \le \theta, \\ 0 \ \ if \ \ t > \theta \end{cases} \tag{3}$$

The fuselink temperature is given by,

$$\Delta\theta(t)=\begin{cases}P_m\sum\limits_{i=1}^{k}r_i\left(1-e^{-\frac{t}{\tau_i}}\right) & if \quad 0<t\le\theta,\\ P_m\left[\sum\limits_{i=1}^{k}r_i e^{-\frac{t-\theta}{\tau_i}}\left(1-e^{-\frac{t}{\tau_i}}\right)\right] & if \quad t>\theta\end{cases} \tag{4}$$

Fig. 4b shows the rectangular pulse series and the equation (5) describes this kind of input power.

$$P(t)=\begin{cases}P_m & if \quad nT\le t\le nT+\theta,\\ 0 & if \quad nT+\theta<t\le(n+1)T\end{cases} \tag{5}$$

The thermal response is given by the following equation (6). For a very big number of rectangular pulses, actually $n\to\infty$, it gets the relation (7).

$$\Delta\theta_{(n+1)}(t)=\begin{cases}P_m\sum\limits_{i=1}^{k}r_i\left[1-\dfrac{e^{-\frac{t-nT}{\tau_i}}\left(1-e^{-\frac{(n+1)T}{\tau_i}}\right)-\left(1-e^{-\frac{nT}{\tau_i}}\right)e^{-\frac{T-\theta}{\tau_i}}}{1-e^{-\frac{T}{\tau_i}}}\right] & if \quad nT\le t\le nT+\theta,\\ P_m\sum\limits_{i=1}^{k}r_i e^{-\frac{t-nT-\theta}{\tau_i}}\dfrac{1-e^{-\frac{\theta}{\tau_i}}}{1-e^{-\frac{T}{\tau_i}}}\left(1-e^{-\frac{(n+1)T}{\tau_i}}\right) & if \quad nT+\theta<t\le(n+1)T\end{cases} \tag{6}$$

$$\Delta\theta_{\infty}(t)=\begin{cases}P_m\sum\limits_{i=1}^{k}r_i\left(1-e^{-\frac{t}{\tau_i}}\right)\dfrac{1-e^{-\frac{T-\theta}{\tau_i}}}{1-e^{-\frac{T}{\tau_i}}} & if \quad nT\le t\le nT+\theta,\\ P_m\sum\limits_{i=1}^{k}r_i e^{-\frac{t-\theta}{\tau_i}}\dfrac{1-e^{-\frac{\theta}{\tau_i}}}{1-e^{-\frac{T}{\tau_i}}} & if \quad nT+\theta<t\le(n+1)T\end{cases} \tag{7}$$

A partial sinusoidal pulse series waveform is shown in Fig. 4c. The equation which describes this type of waveform is given by (8).

$$P(t)=\begin{cases}P_m\sin(\omega t+\gamma) & if \quad nT\le t\le\theta+nT,\\ 0 & if \quad \theta+nT<t\le(n+1)T\end{cases} \tag{8}$$

In order to establish the fuselink temperature when $n\to\infty$, it will use the relation (9), where the notations for φ, Z and δ are described in the expressions (10).

$$\Delta\theta_\infty(t)=\begin{cases} P_m\left\{Z\sin(\omega t+\gamma-\delta)-\sum_{i=1}^{k}r_i\left[\sin(\gamma-\varphi_i)-\sin(\gamma-\varphi_i+\omega\theta)e^{-\frac{T-\theta}{T_i}}\right]\dfrac{e^{-\frac{t}{T_i}}}{\left(1-e^{-\frac{T}{T_i}}\right)\sqrt{1+(\omega T_i)^2}}\right\} \\ if \quad nT\le t\le\theta+nT, \\ P_m\sum_{i=1}^{k}r_i\left[\sin(\omega\theta+\gamma-\varphi_i)-\sin(\gamma-\varphi_i)e^{-\frac{\theta}{T_i}}\right]\dfrac{e^{-\frac{t-\theta}{T_i}}}{\left(1-e^{-\frac{T}{T_i}}\right)\sqrt{1+(\omega T_i)^2}} \\ if \quad \theta+nT<t\le(n+1)T \end{cases} \tag{9}$$

$$ctg\varphi_i=\frac{1}{\omega T_i};\quad Z^2=\sum_{i=1}^{k}(r_i\cos^2\varphi_i)^2+\sum_{i=1}^{k}\left(\frac{r_i}{2}\sin 2\varphi_i\right)^2;\quad tg\delta=\frac{\sum_{i=1}^{k}\frac{r_i}{2}\sin 2\varphi_i}{\sum_{i=1}^{k}r_i\cos^2\varphi_i} \tag{10}$$

From the previous obtained equations to be used for the computation of the temperature rise of the fuselink of the fast fuse in the case of different type of loads, it is easily to be observed that on the one hand the calculations using the analytical formula are not so facile, and on the other hand, it needs to know the thermal resistances r_i and the thermal constants T_i from the exponential decomposition of the transient thermal impedance Z_{th}. As mentioned before, this can be done through experimental tests for a certain fast fuse. Therefore, in order to obtain faster the fuselink temperature rise at different type of thermal loads and also the temperature variation in any other component part of the fast fuse assembly, the solution is to use numerical methods as finite element method.

3. THERMAL MODELLING AND SIMULATIONS

A three-dimensional model for a fast fuse has been developed using a specific software, the Pro-ENGINEER, an integrated thermal design tool for all type of accurate thermal analysis on devices. The subject was a fast fuse type aR with rated current by 400A, rated voltage about 700V and rated power losses of 65W [25]. The 3D model had taken into consideration all the component parts of a fast fuse: outer cap, end tag, rivet, inner cap, ceramic body, fuselink and granular quartz, as shown in Fig. 5. It was considered a simplified geometry for the rivets.

Using this thermal model of the fast fuse, it has been included the busbar terminals as part of a bidirectional rectifier bridge equiped with power diodes, Fig. 6. Taking into account that the rated power losses for the fuse is about 65W and the rated current is 400A, the rated resistance will be,

$$R_n=\frac{P_n}{I_n^2}=0.4m\Omega \tag{11}$$

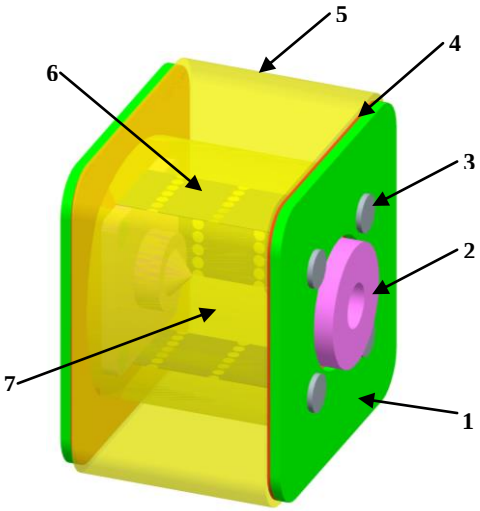

Fig. 5 Geometrical model of the fast fuse (1 – outer cap; 2 – end tag; 3 – rivet; 4 – inner cap; 5 - ceramic body; 6 – fuselink; 7 – granular quartz)

When the considered fast fuse is protecting in series the power semiconductor from the bidirectional rectifier bridge, during normal operating conditions, at a current with the value of 315A results a power losses by,

$$P = R_n \cdot I^2 = 39.69W \tag{12}$$

In this case, because the fuse has three fuselink elements and assuming an equal distribution of the current flow, every fuselink will dissipate 13.23W. The analyzed fuse has the following overall dimensions: length: 50mm, square cross-section: 59mm x 59mm, end tag diameter: 24mm. The fuselink has a length of 38mm, width: 15mm, thickness: 0.15mm, notch diameter: 2.3mm and its thermal time constant is about 12ms [24].

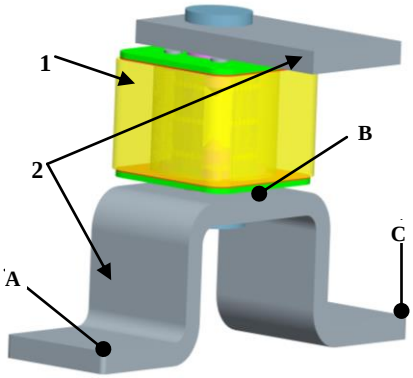

Fig. 6 Geometrical model of the fast fuse assembly (1 – fast fuse; 2 – busbar connections)

The material properties of every component part of the fuse are described in the Table 1. The heat load has been applied on surfaces of the fuselink elements, 13.23W on every one. It is a uniform spatial distribution on these surfaces. The ambient temperature has been considered about 25ºC. From experimental tests it was computed the convection coeffcient k_t = 14.24W/m^{2o}C, for this type of fast fuse [24]. The convection coefficient has been applied on surfaces of outer caps, end tags, rivets, ceramic body and busbar connections with a uniform spatial variation and a bulk temperature of 25ºC.

Table 1 Material data and coefficients at 20ºC

Parameter	Material (and correspondence with the components from Fig.5)					
	Ceramic body (5)	Copper (1, 2)	Iron FE40 (3)	Granular quartz (7)	Silver (6)	Insulation material /pressed carton (4)
ρ (kg/m^3)	2400	8900	7190	1500	8210	1400
c (J/kgºC)	1088	387	420.27	795	377	0.099
λ (W/mºC)	1	385	52.028	0.325	121.22	0.063

Because during analyzed situation, the temperature on the surface of the ceramic body of the fuse or on the surface of the busbars has not increased so much (a maximum of 33°C) in comparison of the initial temperature (the ambient one, about 25°C), it has been considered that the convection coefficient has a constant value which not depends on the temperature variation. For all thermal simulations a 3D finite elements Pro-MECHANICA software has been used. The mesh of this 3D fuse thermal model has been done using tetrahedron solids element types with the 62544 elements and 14322 nodes. The single pass adaptive convergence method to solve the thermal steady-state simulation has been used.

Then, it has been made some steady-state thermal simulations for the fast fuse together with its busbar connections. The temperature distribution inside the fuse and through fuselink elements is shown in the Fig. 7. The maximum temperature, on the fuselinks is 177.6ºC and the minimum, on the surface of busbar connections, is about 28.34ºC.

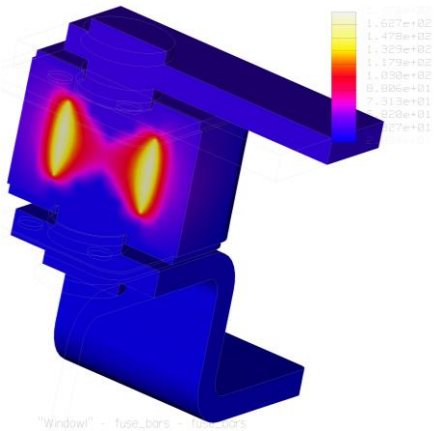

Fig. 7 Temperature distribution through the fuse structure at 50% cross section

Much more, the temperature distribution along the bottom busbar connection mounted on the fuse terminals, has been computed, Fig. 8. It has been considered the temperature along the curve bounded by the points A, B and C. It can be observed a maximum value in the middle of the busbar and the minimum temperatures at the ends. Hence, it results that busbar connections act like a heatsink for the fast fuse. It actually spreads the fuse heating from the middle to the end parts through the busbars to the environment. In order to validate the thermal simulation results, some experimental tests have been performed. It can be noticed that the experimental values at the ends of the busbar are higher than the middle point where actually, the simulated and the experimental value are very close (32.26, respect to 32.3°C). This can be explained because at the ends of the busbar there are connections to the power supply of the uncontrolled bridge rectifier. Actually, these terminal connections act as additional power losses for the busbar.

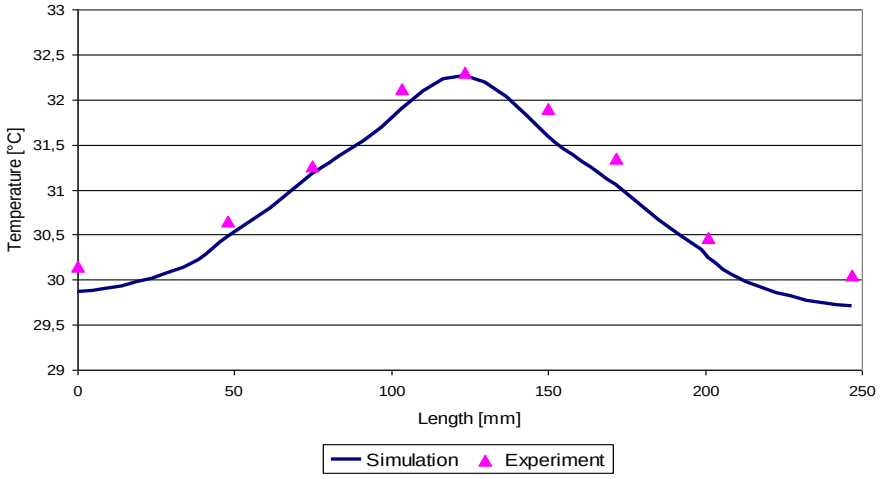

Fig. 8 Temperature distribution along the bottom busbar connection (curve bounded by A, B and C points). Comparison between simulation and experimental tests

Further on, the thermal simulations have been done in order to compute the maximum temperature of the fuselink in both cases with and without busbar connections and for different type of loads presented in the next picture, Fig. 9. It took into account that usually, a fast fuse has to protect against short-circuits power semiconductors as diodes or thyristors from different types of power rectifiers. Hence, it has been considered the following type of thermal loads only in the case of single-phase circuit: one-way uncontrolled bridge rectifier (Fig. 9a), bidirectional uncontrolled bridge rectifier (Fig. 9b), one-way controlled bridge rectifier (Fig. 9c - 135 electrical degrees firing angle) and bidirectional controlled bridge rectifier (Fig. 9d - 135 electrical degrees firing angle). The P_m means the maximum of power loss and for each fuselink is about 18.71W and T is the period of the sinusoidal waveform at 50Hz, so its value is 20ms.

After all of these thermal simulations, the results related to the maximum temperatures for the fast fuse without busbar connections and in the situation when the fuse has mounted the busbar terminals, are synthesized in the Table 2.

It can be noticed that the higher values for the maximum temperature are in the case of fuse without busbar connections. Also, the highest value for temperature is obtained in the case when the thermal load corresponds to the bidirectional uncontrolled bridge rectifier. Actually, this is the situation of the sigle-phase bridge rectifier made with power diodes. The minimum value for temperature, 97.6°C is obtained for the fuse with busbar connections and when the thermal load has the time variation of a single-phase one-way controlled bridge rectifier for 90 firing angle. This is the case of the single-phase rectifier made with thyristors. It is to observe that for a higher firing angle (i.e. 135°el) the maximum temperature is increased (103.7°C for an one-way controlled bridge rectifier and 152.8°C for a bidirectional controlled bridge rectifier, both in the case with busbar connection).

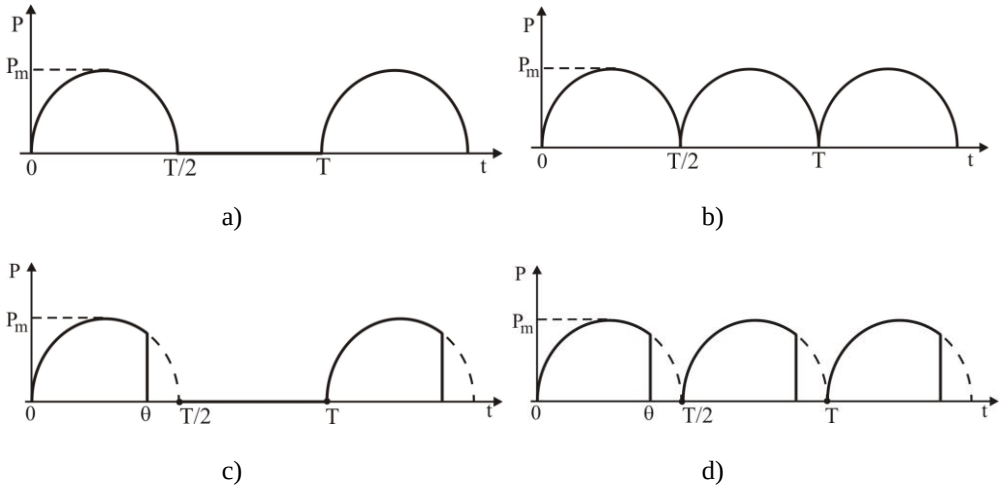

Fig. 9 Different types of thermal load (a - one-way uncontrolled bridge rectified; b - bidirectional uncontrolled bridge rectifier; c - one-way controlled bridge rectifier; d - bidirectional controlled bridge rectifier)

Table 2 Comparison between maximum temperatures

Load type	Maximum temperatures [°C]	
	Without busbars	With busbars
one-way uncontrolled bridge rectified	164.3	115.5
one-way uncontrolled bridge rectified – RMS value	160.2	110.8
bidirectional uncontrolled bridge rectifier	225.5	177.6
bidirectional uncontrolled bridge rectifier – RMS value	220.5	173.5
one-way controlled bridge rectifier (θ = 135°el)	154.3	103.7
one-way controlled bridge rectifier (θ = 135°el) – RMS value	150.1	98.2
bidirectional controlled bridge rectifier (θ = 135°el)	205.5	152.8
bidirectional controlled bridge rectifier (θ = 135°el) – RMS value	202.5	147.8
one-way controlled bridge rectifier (θ = 90°el)	148.2	97.6
one-way controlled bridge rectifier (θ = 90°el) – RMS value	143.2	91.5
bidirectional controlled bridge rectifier (θ = 90°el)	198.8	146.5
bidirectional controlled bridge rectifier (θ = 90°el) – RMS value	195.4	140.2

Hence, for a higher firing angle in the case of controlled power semiconductor devices, the maximum temperature on the fuselinks becomes higher. Also, for the same type of thermal loads, it has been performed the thermal simulations considering the thermal load as a constant value equal with its RMS value. It can be noticed that all obtained values are smaller than the first analyzed case when it has been considered the wave-shape of each thermal load. Therefore, the calculus of the maximum temperatures taking into account only the RMS value of the thermal load, does not give satisfactory results.

The thermal analysis can be extended for other type of thermal load variations, for instance those specific to three-phase power rectifiers when the power semiconductors are diodes or controlled thyristors. Therefore, for a certain power rectifier can be established the thermal stress for fast fuse included all busbar connections and also for the protected device, the power semiconductor. More, it can be analyzed the thermal behaviour of other type of power semiconductor equipment as inverters or frequency converters.

4. CONCLUSIONS

Thermal response of fast fuses for a variety of one-shot and repetitive pulse inputs have been computed with the aim to offer valuable formulae for power circuit designers. A transient thermal calculation using the analytical formula is very complex and difficult to do. So, a more exactly and efficiently thermal calculation of fuses at different types of thermal loads, can be done using specific modelling and simulation software packages based on finite element method. In this way it can be computed the temperature values anywhere inside or on the fast fuse assembly.

The proposed three-dimensional thermal model has been included all the necessary components for a fast fuse such as outer caps, end tags, rivets, inner caps, ceramic body, fuselink elements and granular quartz; also, the simulations have been considered all the thermal model not parts of it or cross-sections.

It can be concluded that in all analysed cases, highest maximum temperature has been obtained for the fast fuse without busbar terminal connections. This is because the busbar connections act like some hetasinks on the surface of the end caps. Hence, these terminals being made from copper have a good thermal conductivity and through the thermal convection they spread the fuse heating in the environment. Also, the maximum temperature of the fast fuse structure depends also on the load types, with the highest value in the case of bidirectional uncontrolled bridge rectifier and minimum for the situation when the load had the waveform variation specific for a thyristor in conduction for a certain time period in the case of one-way rectifier.

Using the 3D simulation software it may improve the fast fuse designing and also there is the possibility to get new solutions for a better protection of power semiconductor devices.

REFERENCES

[1] G. Hoffmann and U. Kaltenborn, "Thermal Modelling of High Voltage H.R.C. Fuses and Simulation of Tripping Characteristic", In Proceedings of the 7th International Conference on Electric Fuses and their Applications. Gdansk, Poland, 2003, pp. 174–180.

[2] M. Wilniewczyc, P.M. McEwan and D. Crellin, "Finite-Element Analysis of Thermally-Induced Film de-Bonding in Single and Two-Layer Thick-Film Substrate Fuses", In Proceedings of the 6th International Conference on Electric Fuses and their Applications. Torino, Italy, 1999, pp. 29–33.

[3] R. K. Huang and S. Nilsson, "Fuse Selection Criteria for Safety Applications," In Proceedings of the 2012 IEEE Symposium on Product Compliance Engineering (ISPCE). Portland OR, USA, 5-7 November 2012, pp. 1–8.
[4] W. Bussiere, "Electric Fuses Operation, a Review: 1. Pre-arcing period", In Proceedings of the IOP Conference Series: Materials Science and Engineering, 2012, vol. 29, no. 1, p. 012001.
[5] W. Bussiere, "Electric Fuses Operation, a Review: 2. Arcing period". In Proceedings of the IOP Conference Series: Materials Science and Engineering, 2012, vol. 29, no. 1, p. 012002.
[6] M. Naidu, S. Gopalakrishnan, and T. W. Nehl, "Fault-Tolerant Permanent Magnet Motor Drive Topologies for Automotive x-by-Wire Systems", *IEEE Trans. on Ind. App*., vol. 46, no. 2, pp. 841–848, January 2010.
[7] D. W. Schlegel, D. Neeser, L. Verstegen and N. Lemberg, "Characteristics, Selection Guidelines and Performance of Circuit Protection Devices for ASDs", In Proceedings of the 2013 IEEE Industry Applications Society Annual Meeting. Lake Buena Vista, FL, USA, December 2013, pp. 1–22.
[8] M. K. Alam, F. H. Khan, J. Johnson and J. Flicker, "PV faults: Overview, Modeling, Prevention and Detection Techniques", In Proceedings of the 2013 IEEE 14th Workshop on Control and Modeling for Power Electronics (COMPEL). Salt Lake City, USA, 2013, pp. 1–7.
[9] S. Madhusoodhanan, D. Patel, S. Bhattacharya, J. A. Carr and Z. Wang, "Protection of a Transformerless Intelligent Power Substation", In Proceedings of the 2013 4th IEEE International Symposium on Power Electronics for Distributed Generation Systems (PEDG). Rogers, AR, USA, 2013, pp. 1–8.
[10] D. M. Bui, S. L. Chen, C. H. Wu, K. Y. Lien, C. H. Huang and K. K. Jen, "Review on Protection Coordination Strategies and Development of an Effective Protection Coordination System for DC Microgrid", In Proceedings of the 2014 IEEE PES Asia-Pacific Power and Energy Engineering Conference (APPEEC). Hong Kong, China, 2014, pp. 1–10.
[11] S. Memiaghe, W. Bussière and D. Rochette, "Numerical Method for Prearcing Times: Application in HBC Fuses with Heavy Fault-Currents", In Proceedings of the Conference on Electric Fuses and Their Application (ICEFA), Clermont-Ferrand, France, 2007, pp. 127–132.
[12] S-H Lee, "Application of High Voltage Current Limiting Fuse Model Using ATP-Draw", *IEEE Trans. on Dielectr. Electr. Insul*., vol. 17, no. 6 , pp. 1806–1813, December 2010.
[13] H. F. Farahani and M. Sabaghi, "Analysis of Current Harmonic on Power System Fuses Using ANSYS", *Indian Journal of Science and Technology*, vol. 5.3, pp. 2396–2400, 2012.
[14] C. Cañas, L. Fernández and R. González, "Minimum Breaking Current Obtaining in Fuses", Proceedings of the 6th Internatinal Conference on Electric Fuses and their Applications. Torino, Italy, 1999, pp. 69–74.
[15] K. Jakubiuk and W. Aftyka, "Heating of Fuse-Elements in Transient and Steady-State", In Proceedings of the 7th International Conference on Electric Fuses and their Applications. Gdansk, Poland, 2003, pp. 181–187.
[16] L. O. Eriksson, D. E. Piccone, L. J. Willinger and W. H. Tobin, "Selecting Fuses for Power Semiconductor Devices", *IEEE Ind. Appl. Mag*., vol. 2, pp. 19, 1996.
[17] A. Pleşca, "Numerical Thermal Analysis of Fuses for Power Semiconductors", *Electr. Pow. Syst. Res*., vol. 83, no. 1, pp. 144–150, 2012.
[18] J. L. Soon and D. D. C. Lu, "Design of Fuse–MOSFET Pair for Fault-Tolerant DC/DC Converters", *IEEE Trans. Power Electron*., vol. 31, no. 9, pp. 6069–6074, February 2016.
[19] P. Nuutinen, P. Peltoniemi and P. Silventoinen, "Short-circuit protection in a converter-fed low-voltage distribution network", *IEEE Trans. Pow.Electron*., vol. 28, no. 4, pp. 1587–1597, 2013.
[20] W. Zhang, D. Xu, P. N. Enjeti, H. Li, J. T. Hawke and H. S. Krishnamoorthy, "Survey on Fault-Tolerant Techniques for Power Electronic Converters", *IEEE Trans. Power Electron*., vol. 29, no. 12, pp. 6319–6331, February 2014.
[21] M. Gleissner and M. M. Bakran, "A Real-Life Fuse Design for a Fault-Tolerant Motor Inverter", In Proceedings of the 18th European Conference on Power Electronics and Applications (EPE'16 ECCE Europe). Karlsruhe, Germany, 2016, pp. 1–11.
[22] S. Mirsaeidi, X. Dong, S. Shi and D. Tzelepis, "Challenges, Advances and Future Directions in Protection of Hybrid AC/DC Microgrids", *IET Renew. Power Gen.*, vol. 11, no. 12, pp. 1495–1502, November 2017.
[23] F. M. Gatta, A. Geri, S. Lauria, M. Maccioni and F. Palone, "Arc Flash in Large Energy Storage Systems—Hazard Calculation and Mitigation", *IEEE Trans. Ind. Appl*., vol. 54, no. 3, pp. 2926–2933, January 2018.
[24] A. Plesca, "Overcurrent protection systems for power semiconductor installations", *PhD Thesis*, Gheorghe Asachi Technical University of Iasi, 2001.
[25] Ferraz – Shawmut, *Ultra – Fast Fuse*, Datasheet.